

On randomized step sizes in Metropolis–Hastings algorithms

Sebastiano Grazzi^{1*}, Samuel Livingstone^{2*}
and Lionel Riou-Durand³

¹Department of Decision Sciences and BIDSA, Bocconi University,
Via Roentgen 1, City, 20136, Milan, Italy.

²Department of Statistical Science, University College, Gower Street,
London, WC1E 6BT, UK.

³Laboratoire de Mathématiques de l’INSA Rouen Normandie, Avenue
de l’Université, 76801 Saint-Étienne-du-Rouvray, France.

*Corresponding author(s). E-mail(s): sebastiano.grazzi@unibocconi.it;
samuel.livingstone@ucl.ac.uk;
 Contributing authors: lionel.riou-durand@insa-rouen.fr;

Abstract

The performance of Metropolis–Hastings algorithms is highly sensitive to the choice of step size, and miss-specification can lead to severe loss of efficiency. We study algorithms with randomized step sizes, considering both auxiliary-variable and marginalized constructions. We show that algorithms with a randomized step size inherit weak Poincaré inequalities/spectral gaps from their fixed-step-size counterparts under minimal conditions, and that the marginalized kernel should always be preferred in terms of asymptotic variance to the auxiliary-variable choice if it is implementable. In addition we show that both types of randomization make an algorithm robust to tuning, meaning that spectral gaps decay polynomially as the step size is increasingly poorly chosen. We further show that step-size randomization often preserves high-dimensional scaling limits and algorithmic complexity, while increasing the optimal acceptance rate for Langevin and Hamiltonian samplers when an Exponential or Uniform distribution is chosen to randomize the step size. Theoretical results are complemented with a numerical study on challenging benchmarks such as Poisson regression, Neal’s funnel and the Rosenbrock (banana) distribution.

Keywords: Monte Carlo, Metropolis–Hastings, Randomized algorithms, Robust algorithms

1 Introduction

Markov chain Monte Carlo (MCMC) methods are the gold standard for asymptotically unbiased Bayesian inference and consist of simulating a discrete-time Markov chain whose ergodic distribution coincides with the given Bayesian posterior π . Ergodic averages can then be used to estimate expectations with respect to the posterior. Many popular MCMC methods are based on the Metropolis–Hastings algorithm, in which each step of the Markov chain is simulated by proposing a new state according to a candidate Markov kernel and then accepting or rejecting it depending on the ratio of the *target* distribution π evaluated at the current and proposed locations.

The candidate kernel is often parametrized by a step size and algorithm performance crucially depends on this choice: when the step size is too small, the process often behaves like a random walk, while a step size that is too large leads to proposals that are rejected with high probability; in both cases the underlying Markov chain mixes slowly and ergodic averages are inefficient. A key contribution for understanding the trade-off between these regimes is given by diffusion/scaling limits, e.g. [Roberts and Rosenthal \(2001\)](#); [Roberts et al. \(1997\)](#); [Yang et al. \(2020\)](#); [Beskos et al. \(2013\)](#). Scaling limits facilitate analysis of the asymptotic performance of an algorithm in high dimensions and provide simple guidelines for optimally tuning the step size. They also imply an order of complexity of the algorithm with respect to the number of dimensions of the target distribution ([Roberts and Rosenthal 2016](#)).

[Livingstone and Zanella \(2022\)](#) recently showed that the performance of standard gradient-based methods such as the Metropolis-adjusted Langevin algorithm (MALA) and Hamiltonian Monte Carlo (HMC) can deteriorate (exponentially) quickly when the step size is miss-specified. The framework is particularly insightful for explaining practical limitations of MCMC methods for target distributions with a complex geometric structure (such as Neal’s funnel in [Neal 2011](#)), for which it is difficult to identify a global step size that allows the Markov chain to efficiently explore the whole space.

Motivated by this, we identify and explore simple modifications of popular algorithms based on randomizing the step size. We show that this simple modification leads to new methods that are provably less affected when the scale of the step size is miss-specified, while retaining the same complexity when studied in the high-dimensional scaling limit regime. Step size randomization, or *jitter*, has been proposed many times in the literature as a useful heuristic (e.g. [Neal 2011](#)). Here we offer a rigorous analysis, providing clear justifications for both theorists and practitioners.

1.1 Main contributions

We identify two approaches to endowing a Metropolis–Hastings algorithm with a randomized step size: an auxiliary-variable approach and a marginalized approach (following the terminology of [Titsias and Papaspiliopoulos 2018](#)). We highlight that the marginalized approach is always more efficient in terms of asymptotic variance, but show empirically that the auxiliary approach often performs equally well and is a more tractable option. We also illustrate that, under mild conditions, both randomized kernels inherit a weak Poincaré inequality/spectral gap whenever the base kernel has one. In both cases we analyze the spectral gaps as the mismatch between the step size and

the scale of some of the target components becomes large, and show that the randomized step size algorithms are more robust than their base counterparts. In addition to this, we analyze the optimal choice of h through the lens of scaling limits for randomized step size algorithms. We show that the step size randomization does not affect the high-dimensional complexity properties as measured by expected squared jumping distance, but it does in fact suggest an increased optimal acceptance rate when compared to the base algorithms. We illustrate this with two concrete examples in the case of MALA and Hamiltonian Monte Carlo (HMC). We complement our theoretical findings with a comprehensive numerical study, illustrating the benefits of a randomized step size on challenging benchmarks such as Neal’s funnel and the Rosenbrock (banana) distribution.

1.2 Related literature

The robustness to tuning framework considered here was introduced in [Livingstone and Zanella \(2022\)](#), where it was used to motivate Metropolis–Hastings algorithms with Barker proposals. In our work, we show that similar robustness properties can also be achieved by randomizing the step sizes of classical algorithms. Scaling limits are a widely used approach in the study of MCMC algorithms, originating in the seminal work [Roberts et al. \(1997\)](#). Our analysis is most closely related to other works directly targeting the expected squared jumping distance (e.g. [Sherlock and Roberts 2009](#); [Vogrinc et al. 2023](#)).

2 MCMC Algorithms with randomized step size

2.1 Metropolis–Hastings algorithms

The Metropolis–Hastings algorithm ([Metropolis et al. 1953](#); [Hastings 1970](#)) is a generic algorithm used to produce a Markov chain $(X_i)_{i=0,1,\dots}$ with limiting distribution equal to a given target distribution π on some space \mathcal{X} . Starting from an initialization X_0 , each random variable $X_{i+1}|(X_i = x)$ is simulated by first drawing a ‘proposal’ y from a candidate Markov kernel $Q_h(x, \cdot)$, which we index by a tuning parameter $h > 0$ (e.g. a step size). Assuming that $\mathcal{X} \subset \mathbb{R}^d$, $\pi(dx) := \pi(x)dx$ and $Q_h(x, dy) := Q_h(x, y)dy$ for all x, y , then $X_{i+1}|(X_i = x)$ is set to be equal to y with probability

$$\alpha_h(x, y) = \min \left(\frac{\pi(y)Q_h(y, x)}{\pi(x)Q_h(x, y)}, 1 \right) \quad (1)$$

whenever $\pi(x)Q_h(x, y) > 0$, and equal to x otherwise. The corresponding Markov transition kernel takes the form

$$P_h(x, dy) = Q_h(x, dy)\alpha_h(x, y) + \left(1 - \int_{\mathcal{X}} Q_h(x, du)\alpha_h(x, u) \right) \delta_x(dy). \quad (2)$$

It is not difficult to verify that P_h is π -invariant for any $h > 0$, since it satisfies the detailed balance condition relative to π , see for example [Roberts and Rosenthal \(2004\)](#) for an overview.

2.2 Randomized step sizes via auxiliary-variable and marginalized kernels

We consider two different approaches to endowing a Metropolis–Hastings kernel P_h with a randomized step size. In both cases the step size will be generated via a distribution $\mu(dz) := \mu(z)dz$ with positive mass on a subset of $(0, +\infty)$, for which we also assume the following.

Assumption 1 *There exists $C > 0$ such that for all $h \geq 1$ and any $z > 0$*

$$\mu(z/h) \geq C\mu(z). \quad (3)$$

Assumption 1 ensures that μ has non-negligible mass near zero, which is important for the spectral gap robustness results of Section 3.

Let $(P_h)_{h>0}$ be the family of Metropolis–Hastings kernels satisfying (2) and indexed by some parameter $h > 0$. We define the *Auxiliary-variable* transition kernel as the mixture

$$\bar{P}_h(x, dy) := \int_0^\infty \mu(z) P_{hz}(x, dy) dz.$$

We can simulate X_{i+1} from $\bar{P}_h(x, \cdot)$ given the current state $X_i = x$ in two simple steps:

1. Sample $z \sim \mu$
2. Sample $X_{i+1} \sim P_{hz}(x, \cdot)$ as in (2).

See Algorithm 1 for more detail.

Algorithm 1 Inner loop Auxiliary-variable MH

Require: $X_i = x \in \mathcal{X}$, $h > 0$, $\mu(\cdot)$, family of kernels $(Q_h)_{h>0}$.

```

1:  $z \sim \mu$ 
2:  $y \sim Q_{hz}(x, \cdot)$ 
3: if  $\text{Unif}([0, 1]) \leq \alpha_{hz}(x, y)$  then
4:    $X_{i+1} = y$ 
5: else
6:    $X_{i+1} = x$ 
7: end if
8: return  $X_{i+1}$ .
```

We also define the *Marginalized* kernel as

$$M_h(x, dy) = \bar{Q}_h(x, y) \tilde{\alpha}_h(x, y) dy + \left(1 - \int_{\mathcal{X}} \bar{Q}_h(x, u) \tilde{\alpha}_h(x, u) du\right) \delta_x(dy) \quad (4)$$

where

$$\bar{Q}_h(x, y) := \int_0^\infty \mu(z) Q_{hz}(x, y) dz$$

and

$$\tilde{\alpha}_h(x, y) = \min \left(\frac{\pi(y) \bar{Q}_h(y, x)}{\pi(x) \bar{Q}_h(x, y)}, 1 \right)$$

is chosen such that each member of the family $(M_h)_{h>0}$ is π -reversible. While M_h always exists, it is only possible to simulate from it when a closed-form expression is available for the transition density \bar{Q}_h . The only difference between the auxiliary-variable kernel \bar{P}_h and the marginalized kernel M_h is in the acceptance probability in Algorithm 1, line 3, which changes from $\alpha_{h,z}(x, y)$ for the auxiliary kernel to $\tilde{\alpha}_h(x, y)$ for the marginalized kernel, for which the variable z has been marginalized.

The auxiliary-variable construction for randomized step sizes has been known and advocated for some time, e.g. [Neal \(2011\)](#) suggests this in the context of Hamiltonian Monte Carlo to avoid proposals being either identical or very close to the current state when the Hamiltonian flow is periodic. To the best of our knowledge, however, there is little rigorous understanding of how this influences the properties of an algorithm.

2.3 Examples of randomized kernels

As shown above, sampling from the auxiliary-variable kernel is a straightforward procedure, but this is not necessarily true for the marginalized kernel M_h . Both the Gaussian random walk Metropolis and the Barker proposal of [Livingstone and Zanella \(2022\)](#) can, however, be derived for example as marginalized versions of simpler base algorithms when the dimension $d = 1$. In the case of the random walk, consider the Metropolis–Hastings algorithm with proposals generated from the current state x via the transformation $y = x + \sqrt{h}\xi$, where $\xi \in \{-1, +1\}$ and $\mathbb{P}(\xi = -1) = 1/2$. Choosing the randomizing distribution μ to be half-Normal, meaning a standard Normal distribution restricted to the positive half-line, means that the marginalized kernel M_h becomes a random walk Metropolis with Gaussian noise of variance h . Similarly, a *Rademacher Barker proposal* algorithm has been discussed in [Vogrinc et al. \(2023\)](#), in which proposals take the form $y = x + b(x, \sqrt{h}\xi) \cdot \sqrt{h}\xi$, with ξ following the same Rademacher distribution and $b(x, \sqrt{h}\xi) \in \{-1, +1\}$ such that $\mathbb{P}(b(x, \sqrt{h}\xi) = +1) := 1/(1 + \exp(-(\log \pi)'(x) \cdot \sqrt{h}\xi))$. Again choosing μ to be half-Normal induces the standard Barker proposal scheme of [Livingstone and Zanella \(2022\)](#), and setting μ to be a Gaussian truncated to be positive with mean $\sqrt{(1 - \sigma^2)}$ and variance σ^2 for some $\sigma < 1$ gives the bi-modal Barker proposal described in Section 4.1 of [Vogrinc et al. \(2023\)](#).

We introduce here two new randomized kernels in the multi-dimensional case, corresponding to marginalized versions of the Metropolis-adjusted Langevin algorithm (MALA), for which the base proposal kernel takes the form

$$Q_h(x, y) = \phi_d(y; x + h\nabla \log \pi(x), 2hI_{d \times d}) \tag{5}$$

where $\phi_d(y; \mu, \Sigma)$ denotes the d -dimensional Gaussian density with mean μ and covariance matrix Σ evaluated at y . The proposal in (5) is justified as it corresponds to an increment of the Euler discretization with step size h of the Langevin diffusion

$$dX_t = \nabla \log \pi(X_t) dt + \sqrt{2}dB_t,$$

which is known to be π -invariant, see [Roberts and Tweedie \(1996\)](#) for details. We identify and analyze two families of implementable Marginalized kernels (4), which are based on randomizing the step size of the MALA kernel in (5). The first modification is when μ is a uniform distribution on $[0, 1]$. In this case,

$$\bar{Q}_h(x, y) \propto e^c \check{K}_{1-d/2}(a, b), \quad (6)$$

where $a = \|y - x\|^2/(4h)$, $b = h\|\nabla \log \pi(x)\|^2/4$, $c = \langle y - x, \nabla \log \pi(x) \rangle/2$ and $\check{K}_\nu(a, b) = \int_1^\infty t^{-\nu-1} \exp(-at - b/t) dt$ is the upper incomplete modified Bessel function of the second kind. When the dimension d is odd, (6) can be re-expressed in terms of the complementary error function.

The second version is when μ follows an $\text{Exp}(1)$ distribution, leading to

$$\bar{Q}_h(x, y) \propto e^c \left(\frac{a}{b}\right)^{\frac{1}{2}-\frac{d}{4}} K_{1-d/2}(2\sqrt{ab}),$$

where $a = \|y - x\|^2/(4h)$, $b = 1 + h\|\nabla \log \pi(x)\|^2/4$, $c = \langle y - x, \nabla \log \pi(x) \rangle/2$ and $K_\nu(x)$ is the modified Bessel function of the second kind, which is readily computable by standard scientific programming languages. More generally, whenever μ is chosen as an instance of the Generalized Inverse Gaussian (GIG) family, then the marginalized kernel will follow a generalized hyperbolic distribution, with density expressed in terms of a modified Bessel function as above ([Jørgensen 2012](#)). Other natural choices for μ within the GIG family are Gamma, inverse Gamma and inverse Gaussian distributions. We compare both of these new marginalized algorithms to their auxiliary and base counterparts in Section 5.

3 Spectral gap analysis

We present here several results related to Auxiliary-variable and Marginalized Metropolis–Hastings transition kernels. We first consider Dirichlet forms, comparing the kernels to each other and P_h , and also showing in Section 3.3 that for any base kernel P_h both \bar{P}_h and M_h will attain the ‘robustness to tuning’ property that spectral gaps decay at a polynomial rate in h^{-1} as $h \uparrow \infty$ ([Livingstone and Zanella 2022](#)). Crucially, this robustness analysis requires no assumptions on the target distribution other than that P_1 possesses a spectral gap. In the absence of this, our conclusions could also be modified to the case of weak Poincaré inequalities using the results of [Andrieu et al. \(2022\)](#). We also note that the results hold in general for any Markov kernel indexed by a one-dimensional parameter h , and therefore extend to other cases than when h is the algorithmic step size.

3.1 Dirichlet forms, Poincaré inequalities & spectral gaps

For any $f : \mathcal{X} \rightarrow \mathbb{R}$, and any π -reversible Markov kernel P , we define an associated Dirichlet form

$$\mathcal{E}(P, f) := \frac{1}{2} \int (f(y) - f(x))^2 \pi(dx) P(x, dy).$$

Let $L_0^2(\pi) := \{f : \mathcal{X} \rightarrow \mathbb{R} \mid \int f(x)^2 \pi(dx) < \infty, \int f(x) \pi(dx) = 0\}$. The Markov chain $\{X_n\}_{n \in \mathbb{N}}$ with transition kernel P satisfies a *Poincaré inequality* with Poincaré constant $c \in (0, \infty)$ if for all $f \in L_0^2(\pi)$

$$\text{Var}_\pi(f) \leq c\mathcal{E}(P, f). \quad (7)$$

The (right) *spectral gap* for P is then defined as

$$\text{Gap}(P) = \inf_{f \in L_0^2(\pi)} \frac{\mathcal{E}(P, f)}{\text{Var}_\pi(f)}.$$

It is straightforward to see that $1/\text{Gap}(P)$ is the smallest choice of c for which (7) can hold. For any kernel P the corresponding Markov operator P , defined point-wise as $Pf(x) := \int f(y)P(x, dy)$ for any $f \in L_0^2(\pi)$, is called positive if it has a spectrum that is wholly contained in $[0, 1]$. If P is a positive operator and (7) holds then for any $f \in L_0^2(\pi)$

$$\text{Var}_\pi(Pf) \leq (1 - \text{Gap}(P))^2 \cdot \text{Var}_\pi(f).$$

From this equation, geometric convergence in total variation distance towards equilibrium can be deduced. Precisely, noting for any signed measure μ that $\|\mu\|_{TV} := \sup_{f: \mathcal{X} \rightarrow [0, 1]} |\mu(f)|$, it holds that

$$\|\mu P^n - \pi\|_{TV} \leq \frac{1}{2} \chi^2(\mu || \pi)^{1/2} \cdot (1 - \text{Gap}(P))^n,$$

where $\mu P(\cdot) := \int \mu(dx)P(x, \cdot)$ and $\chi^2(\mu || \pi) := \int ((d\mu/d\pi)(x) - 1)^2 \pi(dx)$ denotes the χ^2 -divergence between μ and π . In words, if the chain is initialized from a probability distribution μ , then the distance to equilibrium decays geometrically with rate $(1 - \text{Gap}(P))$, and the distance also depends on how close μ is to the limiting distribution π . When P is not positive then it can be replaced with its lazy counterpart $(P + I)/2$.

The spectral gap can also be related to the asymptotic variance of ergodic averages. Indeed if $\{X_1, X_2, X_3, \dots\}$ is a Markov chain with transition kernel P and $X_0 \sim \pi$ then for any $g \in L_0^2(\pi)$ it holds that

$$\lim_{n \rightarrow \infty} \frac{1}{n} \text{Var} \left(\sum_{i=1}^n g(X_i) \right) \leq \left(\frac{2}{\text{Gap}(P)} - 1 \right) \text{Var}_\pi(g).$$

This can be seen by first noting that if $\text{Gap}(P) > 0$ then the asymptotic variance for g can be written $2\mathcal{E}(P, h_g) - \text{Var}_\pi(g)$, where h_g solves the Poisson equation $(I - P)h_g = g$ (e.g. [Roberts and Rosenthal 2004](#)), and then noting that in this case the Dirichlet form can be straightforwardly re-expressed as $\mathcal{E}(P, h_g) = \int g(x)h_g(x)\pi(dx)$. The Cauchy–Schwarz inequality therefore implies that $\mathcal{E}(P, h_g) \leq \sqrt{\text{Var}_\pi(g)}\sqrt{\text{Var}_\pi(h_g)}$, and applying the Poincaré inequality (7) to $\sqrt{\text{Var}_\pi(h_g)}$ with the constant $c = 1/\text{Gap}(P)$ gives upon rearrangement the inequality $\mathcal{E}(P, h_g) \leq \text{Var}_\pi(g)/\text{Gap}(P)$. Substituting into the asymptotic variance expression gives the result.

In many settings a Markov chain does not have a positive spectral gap, or equivalently a Poincaré inequality does not hold. In this case Dirichlet forms can still be used to understand the properties of the Markov chain via a *weak Poincaré inequality*

$$\text{Var}_\pi(f) \leq s\mathcal{E}(P, f) + \beta(s)\Phi(f), \quad (8)$$

for some $s > 0$ and suitable real-valued functions β and Φ (which must also satisfy additional conditions, see e.g. Section 2.2.1 of [Andrieu et al. 2022](#)). It can be shown that if (8) holds then the Markov chain converges to equilibrium at a rate that is connected to the functions β and Φ (see e.g. [Andrieu et al. 2022](#)).

3.2 Orderings and Robustness to tuning

Markov chains can be compared in various ways. The approach introduced by Peskun ([Peskun 1973](#)) is to construct a partial order on π -reversible Markov transition kernels. If P_1 and P_2 are two such kernels then $P_1 \succeq P_2$ in the sense of Peskun if $P_1(x, A \cap \{x\}^c) \geq P_2(x, A \cap \{x\}^c)$ for all $x \in \mathcal{X}$ and any event A . Peskun showed that when \mathcal{X} is finite such an ordering implies that asymptotic variances computed using ergodic averages from P_1 will be smaller than those computed from P_2 for any square-integrable test function g . Tierney ([Tierney 1998](#)) then extended this result to general state spaces. It is not difficult to see that if $P_1 \succeq P_2$ then $\mathcal{E}(P_1, f) \geq \mathcal{E}(P_2, f)$ for all $f \in L_0^2(\pi)$, from which it is natural to consider directly ordering Dirichlet forms. The same asymptotic variance conclusion holds under this ordering owing to its Dirichlet form representation given in the previous section.

The criterion of Peskun, often called ‘off-diagonal domination’, can be too stringent to be satisfied in many applications, and applies only to reversible Markov chains. It has been extended in various directions, see e.g. [Mira and Geyer \(1999\)](#); [Andrieu and Livingstone \(2021\)](#). One useful generalization for our purposes is to consider for some $\omega > 0$ the relaxation

$$\mathcal{E}(P_1, g) \geq \omega \mathcal{E}(P_2, g). \quad (9)$$

This weakened ordering implies that $\text{Gap}(P_1) \geq \omega \text{Gap}(P_2)$, and also that asymptotic variances under P_1 are less than those under P_2 up to a constant additive term depending on ω ([Andrieu et al. 2018](#)). In addition [Andrieu et al. \(2022\)](#) show that in the absence of a spectral gap conditions such as (9) can be used to establish that a weak Poincaré inequality holds for P_1 provided that such an inequality holds for P_2 .

The ordering (9) was used in [Livingstone and Zanella \(2022\)](#) to assess the robustness of a Metropolis–Hastings algorithm to the choice of step size. The authors introduce a framework in which the algorithm targets a distribution with density $\pi^{(\lambda)}$, where λ denotes the scale of the first component. Crucially, the same choice of algorithmic step size is chosen for all different values of λ , meaning that as $\lambda \downarrow 0$ the result is an algorithm for which the step size is much larger than the optimal choice, and when $\lambda \uparrow \infty$ it is much smaller than optimal. The authors study the rate at which the spectral gap of the corresponding Markov chain decays to zero as either $\lambda \downarrow 0$ or $\lambda \uparrow \infty$. If the rate is polynomial in $1/\lambda$ as $\lambda \downarrow 0$ then the algorithm is called *robust to tuning*. The authors show that the random walk Metropolis and Barker proposal are robust to tuning as $\lambda \downarrow 0$ while MALA and HMC are not, while all algorithms behave

similarly as $\lambda \uparrow \infty$. They then showcase through numerical experiments that robustness to tuning is a very beneficial property for learning optimal algorithmic tuning parameters using adaptive Markov chain Monte Carlo.

It can be shown that studying the above algorithms with a fixed choice of step size as the target $\pi^{(\lambda)}$ changes in the manner described above is equivalent to studying the algorithms with a fixed target distribution $\pi^{(1)}$ where the algorithmic step size h is allowed to vary. Precisely, there is an isomorphism between the Metropolis–Hastings algorithm with proposal kernel Q_1 targeting $\pi^{(\lambda)}$ and the algorithm with proposal kernel Q_h targeting $\pi^{(1)}$ if $h := 1/\lambda^2$, which implies that the two resulting Markov chains will have the same spectral gap (see the supplement to [Livingstone and Zanella \(2022\)](#) for details). Re-framing the results of [Livingstone and Zanella \(2022\)](#) in these terms, the implication is that for MALA and HMC algorithm performance decays extremely quickly as the step size is increased beyond the optimal choice, meaning that performance is crucially dependent on this parameter. By contrast, in the random walk Metropolis and Barker proposal the decay in efficacy is much less severe. The authors showcase that in the context of learning a step size iteratively through a stochastic approximation scheme depending on the Markov chain samples, as is commonly done in practice, if the sample quality is still adequate when the step size is larger than optimal then this can facilitate much faster optimization.

MALA and the Barker proposal ([Livingstone and Zanella 2022](#); [Hird et al. 2020](#); [Vogrinc et al. 2023](#)) are natural comparators using this framework since the step sizes in both algorithms clearly have the same physical meaning. Both are Metropolis–Hastings algorithms in which the proposal can be constructed by numerically integrating the overdamped Langevin diffusion for a fixed time-step, and then applying a Metropolis–Hastings filter to correct for discretisation bias at equilibrium. In the case of the Langevin algorithm this fact is well-known and the numerical scheme is the classical Euler–Maruyama method. In the Barker case the numerical scheme is the skew-symmetric method introduced in [Iguchi et al. \(2024\)](#). In both cases the step size h corresponds to the physical time for which the diffusion process is integrated forward to generate a proposal. What is clear from the results of [Livingstone and Zanella \(2022\)](#) is that the rate at which the numerical scheme becomes unstable is different between the two algorithms.

3.3 Spectral gap results for kernels with randomized step size

We now present ordering and robustness results for Metropolis–Hastings algorithms with a randomized step size, considering both the auxiliary-variable and marginalized approaches introduced in Section 2.2. We begin with a direct ordering.

Proposition 1 *For any $f \in L_0^2(\pi)$, any $h > 0$ and any base kernel P_h we have*

$$\mathcal{E}(M_h, f) \geq \mathcal{E}(\bar{P}_h, f),$$

from which it follows that

$$\text{Gap}(M_h) \geq \text{Gap}(\bar{P}_h),$$

and that an ergodic average constructed using M_h will always have smaller asymptotic variance than the same ergodic average using \bar{P}_h .

This result follows directly from Proposition 1 of [Titsias and Papaspiliopoulos \(2018\)](#), see also [Storvik \(2011\)](#). The practical conclusion is that if the marginalized kernel is tractable then this should always be preferred. We show in Section 5, however, that the difference in performance appears to be very small in many practical cases of interest, so as to be essentially indiscernible.

Using the above, we can compare both M_h and \bar{P}_h to the base kernel P_h in terms of spectral gaps. We begin with the following assumption on P_h .

Assumption 2 *The kernel P_h satisfies one of the following conditions:*

(i) *(Weak Poincaré inequality) There is a μ -measurable $H \subset (0, \infty)$ such that for any $h \in H$ the weak Poincaré inequality*

$$\text{Var}_\pi(f) \leq c(h)\mathcal{E}(P_h, f) + \beta(c(h))\Phi(f)$$

holds with $0 < c(h) < \infty$, for suitable functions β and Φ .

(ii) *(Poincaré inequality) Part (i) holds with $\beta(c(h)) \equiv 0$.*

Assumption 2(ii) implies that for any $h \in H$ the kernel P_h has a positive spectral gap, and that

$$\text{Gap}(P_h) \geq \frac{1}{c(h)}.$$

Provided that either this or Assumption 2(i) is true then some conclusions can be drawn about \bar{P}_h . We begin with a technical result.

Lemma 1 *For any $f \in L_0^2(\pi)$, it holds that*

$$\mathcal{E}(\bar{P}_h, f) = \int \mathcal{E}(P_{hz}, f) \mu(dz). \quad (10)$$

Proof Direct calculation gives

$$\begin{aligned} 2\mathcal{E}(\bar{P}_h, f) &= \int (f(y) - f(x))^2 \pi(dx) \bar{P}_h(x, dy) \\ &= \int (f(y) - f(x))^2 \pi(dx) P_{hz}(x, dy) \mu(dz) \\ &= \int 2\mathcal{E}(P_{hz}, f) \mu(dz) \end{aligned}$$

as required. \square

We can combine Lemma 1 with Assumption 2(i) to conclude a weak Poincaré inequality and Assumption 2(ii) to conclude a positive spectral gap for \bar{P}_h provided that μ gives positive mass to the set $H/h := \{z \in \mathbb{R} : hz \in H\}$, as stated below.

Proposition 2 If Assumption 2(i) holds and $\mu(H/h) > 0$ then \bar{P}_h satisfies a weak Poincaré inequality of the form

$$\text{Var}_\pi(f) \leq c_*(h, \mu)\mathcal{E}(\bar{P}_h, f) + \beta_*(h, \mu)\Phi(f)$$

for any $f \in L_0^2(\pi)$, where

$$c_*(h, \mu)^{-1} := \int_{z \in H/h} \frac{1}{c(hz)}\mu(dz), \quad \beta_*(h, \mu) := c_*(h, \mu) \cdot \int_{z \in H/h} \frac{\beta(c(hz))}{c(hz)}\mu(dz).$$

In the case of Assumption 2(ii) then combining with Proposition 1 implies

$$\text{Gap}(M_h) \geq \text{Gap}(\bar{P}_h) \geq \frac{1}{c_*(h, \mu)}.$$

Proof The weak Poincaré inequality can be re-written

$$\mathcal{E}(P_h, f) \geq c(h)^{-1} [\text{Var}_\pi(f) - \beta(c(h))\Phi(f)].$$

Combining Lemma 1 and Assumption 2(i) therefore gives for any $f \in L_0^2(\pi)$

$$\begin{aligned} \mathcal{E}(\bar{P}_h, f) &\geq \int_{z \in H/h} \mathcal{E}(P_{hz}, f)\mu(dz) \\ &\geq \text{Var}_\pi(f) \int_{z \in H/h} \frac{1}{c(hz)}\mu(dz) - \Phi(f) \int_{z \in H/h} \frac{\beta(c(hz))}{c(hz)}\mu(dz), \end{aligned}$$

from which upon re-arrangement the first part of the result follows. Setting $\Phi(f) \equiv 0$ as in Assumption 2(ii) then implies $\text{Gap}(\bar{P}_h) \geq 1/c_*(h, \mu)$, from which the second part follows. \square

The following immediate corollary highlights the additional robustness that can be offered when randomizing the step size from a suitable μ using either the marginal or auxiliary-variable approach.

Corollary 1 If Assumption 2(ii) holds for some H of positive Lebesgue measure on \mathbb{R} , and the density $\mu(z) > 0$ for all $z \in \mathbb{R}$, then for any $h \in \mathbb{R}$

$$\text{Gap}(M_h) \geq \text{Gap}(\bar{P}_h) > 0.$$

Example 1 When π is Gaussian it is well-known that MALA and Hamiltonian Monte Carlo can only be shown to have a positive spectral gap if h is chosen to be suitably small (Roberts and Tweedie 1996; Livingstone et al. 2019a; Durmus et al. 2020). By contrast both M_h and \bar{P}_h will have a positive spectral gap for any choice of h provided that the randomizing distribution μ has positive density in a neighbourhood of zero.

Proposition 2 already illustrates how the spectral gaps of M_h and \bar{P}_h can be more stable as $h \uparrow \infty$ than that of P_h . To see this, suppose that Assumption 2(ii) is satisfied with $c(h) := e^h$, meaning the spectral gap of P_h decays to zero at an exponential rate as h increases. Choosing μ to be a half-Normal distribution with $\sigma^2 = 1$, then $c_*(h, \mu)^{-1} = 2e^{h^2/2}(1 - \Phi(h))$, where Φ is the standard Normal cumulative distribution function. For large h then $c_*(h, \mu) \sim h\sqrt{\pi/2}$, meaning that the spectral gaps of M_h and \bar{P}_h decay at a slower polynomial rate as $h \uparrow \infty$. In the next result we show that this robustness to tuning holds more generally for the randomized kernels. We

show below that for any Metropolis–Hastings algorithm P_h indexed by some one-dimensional parameter h , the act of randomizing h by using either M_h or \bar{P}_h imposes a level of robustness, even if this is not the case for the original kernel P_h . We begin with a weak ordering of the Dirichlet forms.

Proposition 3 *For any $f \in L_0^2(\pi)$ and any $h > 1$, suppose μ satisfies Assumption 1, then*

$$\mathcal{E}(\bar{P}_h, f) \geq w(h)\mathcal{E}(\bar{P}_1, f), \quad w(h)^{-1} = O(h).$$

Proof Direct calculation and using Assumption 1 gives

$$\begin{aligned} 2\mathcal{E}(\bar{P}_h, f) &= \int (f(x) - f(y))^2 \pi(dx) \int_0^\infty \mu(z) P_{hz}(x, dy) dz \\ &= \int (f(x) - f(y))^2 \pi(dx) \int_0^\infty \mu\left(\frac{u}{h}\right) P_u(x, dy) \frac{1}{h} du \\ &\geq \int (f(x) - f(y))^2 \pi(dx) \int_0^\infty C\mu(u) P_u(x, dy) \frac{1}{h} du \\ &= 2\mathcal{E}(\bar{P}_1, f) \times \frac{C}{h}. \end{aligned}$$

Setting $w(h) := C/h$ therefore establishes the result. \square

Combining Theorem 3 with Theorem 1 leads to the following, which is the main result of this section.

Theorem 4 *If $\text{Gap}(\bar{P}_1) > 0$ and μ satisfies Assumption 1 then*

$$\text{Gap}(M_h) = \Omega(h^{-1}), \quad \text{Gap}(\bar{P}_h) = \Omega(h^{-1}),$$

where $f = \Omega(g) \iff \liminf_{t \rightarrow \infty} f(t)/g(t) > 0$ for $f, g : [0, \infty) \rightarrow [0, \infty)$.

Proof From Theorem 3 and the assumption that $\text{Gap}(\bar{P}_1) > 0$ the result follows for \bar{P}_h . Given that $\text{Gap}(M_h) \geq \text{Gap}(\bar{P}_h)$ by Theorem 1 then this also implies the result for M_h . \square

4 Scaling limits

Scaling limits are classical tools used to understand how the step size h must be chosen as the dimension d of the target distribution π increases to prevent the acceptance rate from degenerating. These results give the algorithmic dependence on d and can be used to optimize the average acceptance rate of the algorithm, providing practical guidance for tuning h in high dimensions.

The general framework makes some regularity assumptions on a sequence of target distributions π_d on \mathbb{R}^d (e.g. being of the product form, although generalizations are possible). Under these assumptions, optimal scaling results show that there exists a constant $c > 0$ such that for all $\ell > 0$, $X \sim \pi_d$, $Y \sim Q_h(X, \cdot)$ and $h_d = \ell d^{-c}$, as $d \rightarrow \infty$,

$$a(d, P_{h_d}) := \mathbb{E}(\alpha(X, Y)) \rightarrow a(\ell) := 2\Phi\left(-\kappa\ell^{1/(2c)}/2\right) \quad (11)$$

where $\kappa > 0$ is a constant whose expression depends on the algorithm. The limit in (11) identifies the appropriate scaling of the step size h such that the average acceptance rate (i.e. the probability that the Markov chain changes its value in one step) has a non-trivial limit in $[0, 1]$. Furthermore, for any two increments of the Markov chain $X_i \sim \pi_d$, $X_{i+1} \sim P_{h_d}(X_i, \cdot)$ and the same constants c, h_d as above, as $d \rightarrow \infty$,

$$\text{ESJD}(d, P_{h_d}) := d^c \mathbb{E} \left[\left(X_i^{(1)} - X_{i+1}^{(1)} \right)^2 \right] \rightarrow \text{eff}(\ell) := \ell a(\ell) \quad (12)$$

where $X^{(j)}$ is the j th element of X ; see [Roberts and Rosenthal \(2001\)](#) for an overview. The quantity on the left hand side of (12) is the (scaled) expected squared jumping distance (ESJD) of the first coordinate. Maximizing ESJD corresponds to minimizing the 1-lag autocorrelation function of the Markov chain $(X_i^{(1)})_{i=1,2,\dots}$, and to reducing the asymptotic variance of ergodic in the high-dimensional limit, see for example [Rosenthal \(2003\)](#). Furthermore, the right-hand side of (12) also corresponds to the speed (or diffusivity) of the Langevin diffusion process obtained as a high-dimensional limit of the (appropriately rescaled) original Markov chain, see [Roberts et al. \(1997\)](#); [Roberts and Rosenthal \(1998\)](#) for details.

If the limits in (11) and (12) hold, one can optimize the function $\text{eff}(\ell)$ and find the optimal asymptotic acceptance rate as follows. Letting $u = \ell^{1/(2c)} \kappa / 2$, the optimal ℓ maximizing the asymptotic ESJD satisfies

$$\begin{aligned} \frac{\partial}{\partial \ell} \text{eff}(\ell) = 0 &\Leftrightarrow 2\Phi(-\ell^{1/(2c)} \kappa / 2) - \frac{\kappa}{2c} \ell^{1/(2c)} \phi(-\ell^{1/(2c)} \kappa / 2) = 0 \\ &\Leftrightarrow \Phi(-u) - \frac{1}{2c} u \phi(-u) = 0 \end{aligned} \quad (13)$$

where ϕ denotes the standard Gaussian density in one dimension. One can then find numerically ℓ_{opt} by solving (13) and compute the optimal asymptotic acceptance rate $a(\ell_{\text{opt}})$.

Classical scaling limits have been established for random walk Metropolis with $c = 1$ and $a(\ell_{\text{opt}}) = 0.234$ ([Roberts et al. 1997](#)), Metropolis-adjusted Langevin algorithm (MALA) and the Barker proposal with $c = 1/3$ and $a(\ell_{\text{opt}}) = 0.574$ ([Roberts and Rosenthal 1998](#); [Vogrinc et al. 2023](#)) and for HMC and Metropolis-adjusted Langevin trajectories with $c = 1/4$ and $a(\ell_{\text{opt}}) = 0.651$ ([Beskos et al. 2013](#); [Riou-Durand and Vogrinc 2022](#)).

Turning now to our randomized algorithms. Our main result below shows that if a scaling limit holds true for a Markov kernel P_h , then similar limits hold for our Auxiliary-variable Markov kernel \bar{P}_h in Algorithm 1.

Theorem 5 (Scaling limits for Auxiliary-variable kernels) *Suppose that for some sequence of kernels P_{h_d} , the limits (11) and (12) hold with $h_d = \ell d^{-c}$, for some $c > 0$. Then, as $d \rightarrow \infty$,*

$$a(d, \bar{P}_{h_d}) \rightarrow \bar{a}(\ell) := \int_0^\infty a(\ell z) \mu(z) dz.$$

Moreover, setting $f_d(z) := \text{ESJD}(d, P_{h_dz})$, assuming that the sequence $f_1(z), f_2(z), \dots$ is uniformly μ -integrable, then

$$\text{ESJD}(d, \bar{P}_{h_d}) \rightarrow \overline{\text{eff}}(\ell) := \int_0^\infty \text{eff}(\ell z) \mu(z) dz.$$

Proof Let $X \sim \pi_d$, $Y \sim Q_{h_dz}(X, \cdot)$. We can use previous optimal scaling results in (11)-(12), to claim that for any $z > 0$, as $d \rightarrow \infty$, we have the point-wise limits

$$\mathbb{E}(\alpha(X, Y)) \rightarrow a(\ell z), \quad \text{ESJD}(d, P_{h_dz}) \rightarrow \text{eff}(\ell z).$$

By taking expectations with respect to z the first part of the theorem is proven by applying the bounded convergence theorem. For the second part note that $\text{ESJD}(d, \bar{P}_{h_d}) = \int \text{ESJD}(d, P_{h_dz}) \mu(dz) = \int f_d(z) \mu(dz)$, so uniform μ -integrability of the sequence f_1, f_2, \dots implies the result by Vitali convergence. \square

The uniform integrability condition can be satisfied for many algorithms of interest. We give some examples in the below proposition.

Proposition 6 *The sequence $f_d(z) := \text{ESJD}(d, P_{h_dz})$ is uniformly integrable in the following cases:*

- (i) P_{h_dz} is the Gaussian random walk Metropolis kernel and μ has finite mean
- (ii) P_{h_dz} is the MALA kernel, μ has finite second moment, and $\pi_d(x) := \prod_{i=1}^d g(x_i)$ with the sequence $\mathbb{E}_{\pi_d}[(\log g)'(X_1)^2]$ uniformly bounded.

Proof In the random walk case note that $\text{ESJD}(d, P_{h_dz}) \leq dhz\mathbb{E}[\xi^2] = \ell z$, where $\xi \sim N(0, 1)$. A straightforward dominating function is therefore $u(z) := \ell z$, which is μ -integrable if μ has finite mean. In the MALA case the jumping distance satisfies

$$\text{ESJD}(d, P_{h_dz}) \leq d^{1/3} \left(h_d^2 z^2 \mathbb{E}[(\log g)'(X_1)^2] + 2h_d z \right) \leq C(z^2 + z)$$

for large enough $C < \infty$ provided that $\mathbb{E}[(\log g)'(X_1)^2]$ is uniformly bounded. The dominating function $u(z) := C(z^2 + z)$ can therefore be chosen to establish the result provided that μ has finite second moment. \square

Theorem 5 implies that, by randomizing the step size, the algorithmic dependence relative to the dimension d stays unchanged.

Moreover, similarly to (13) and by a change of variable $u = z\ell(\kappa/2)^{2c}$, $\bar{\ell}_{\text{opt}} = \arg \max \{\text{eff}(\ell)\}$ now solves

$$\int_0^\infty \left(u\Phi(-u^{1/(2c)}) - \frac{1}{2c} u^{1/(2c)+1} \phi(-u^{1/(2c)}) \right) \mu(u/\omega) du = 0.$$

where $\omega = \bar{\ell}_{\text{opt}}(\kappa/2)^{2c}$, yielding new optimal acceptance rates for Auxiliary-variable Metropolis–Hastings kernels given by

$$\bar{a}(\bar{\ell}_{\text{opt}}) = \int_0^\infty 2\Phi(-(\bar{\ell}_{\text{opt}} z)^{1/(2c)} \kappa/2) \mu(z) dz = \frac{2}{\omega} \int_0^\infty \Phi(-u^{1/(2c)}) \mu(u/\omega) du,$$

μ	MALA ($c = 1/3$)		HMC ($c = 1/4$)	
	$\bar{a}(\bar{\ell}_{\text{opt}})$	$\text{eff}(\ell_{\text{opt}}) / \bar{\text{eff}}(\bar{\ell}_{\text{opt}})$	$\bar{a}(\bar{\ell}_{\text{opt}})$	$\text{eff}(\ell_{\text{opt}}) / \bar{\text{eff}}(\bar{\ell}_{\text{opt}})$
Uniform	0.680	1.342	0.750	1.387
Exponential	0.687	1.758	0.737	1.889

Table 1 Optimal acceptance rate $\bar{a}(\bar{\ell}_{\text{opt}})$ with $\ell_{\text{opt}} = \arg \max_{\ell} \text{eff}(\ell)$ and loss of optimal efficiency $\max(\text{eff}(\ell)) / \max(\bar{\text{eff}}(\ell))$ for the Auxiliary-variable MALA and HMC with Uniform and Exponential randomized step sizes.

see Table 1 for μ equal to both Exponential and Uniform distributions and for MALA (with scale $c = 1/3$) and HMC (with scale $c = 1/4$). Note that these values are larger than the optimal acceptance rate of the original MALA and HMC algorithms.

Note that for all $\ell > 0$,

$$\bar{\text{eff}}(\ell) = \int_0^\infty \text{eff}(\ell z) \mu(z) dz \leq \int_0^\infty \text{eff}(\ell_{\text{opt}}) \mu(z) dz = \text{eff}(\ell_{\text{opt}})$$

where $\ell_{\text{opt}} = \arg \max \text{eff}(\ell)$, therefore, the randomized algorithms have a loss of asymptotic efficiency when ℓ is optimally tuned. We quantify this loss in Table 1 by comparing the maximum of $\text{eff}(\ell)$ and $\bar{\text{eff}}(\ell)$ for the algorithms considered above.

5 Numerical experiments

We illustrate our theoretical results and numerically compare our algorithms on standard benchmark target distributions: Neal’s funnel (Neal 2011) and Rosenbrock’s banana distribution (Pagani et al. 2022). We also numerically show the convergence of our algorithms with initialization in the tails and a Bayesian posterior given by a Poisson regression model. The code for reproducing all the experiments is available at <https://github.com/SebaGraz/RSS>.

5.1 ESJD

We illustrate first the robustness property of our Auxiliary-variable and Marginalized MALA algorithms by comparing their ESJD with that of standard MALA as the step size h varies. ESJD is estimated with $N = 10^6$ Monte Carlo samples and standard Rao–Blackwellization techniques. Figure 1 shows these results for different target distributions (Normal, Laplace, and Student- t). Note that when h is small the performance is almost identical across all algorithms. For large h , however, the ESJD of the randomized algorithms decays more slowly than that of standard MALA, as supported by Theorem 4. Furthermore, as indicated by Proposition 1, Marginalized MALA slightly outperforms Auxiliary-variable MALA in two of the three cases when considering the exponential randomization of the step size. However, for Uniform randomized step sizes, the ESJD of Marginalized and Auxiliary-variable MALA appear indistinguishable.

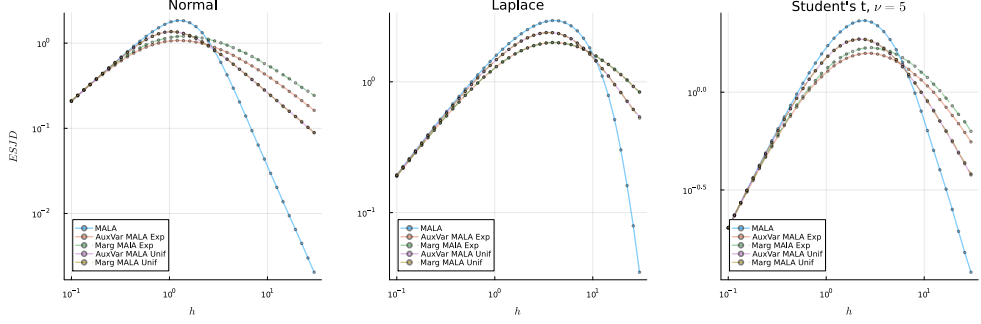


Fig. 1 ESJD estimates (log-scale) as a function of the step size (x -axis, log-scale) of standard MALA (blue), Auxiliary-variable MALA with Exponential (red) and Uniform (purple) randomized step sizes and Marginalized MALA with Exponential (green) and Uniform (yellow) randomized step sizes, for a one-dimensional standard Normal (left), Laplace (center), Student- t with 5 degrees of freedom (right).

5.2 Neal's funnel distribution

The d -dimensional Neal's funnel distribution [Neal \(2011\)](#) is a hierarchical model defined as

$$X_1 \sim \mathcal{N}(0, \sigma^2), \quad X_i \mid X_1 \stackrel{\text{i.i.d.}}{\sim} \mathcal{N}(0, e^{X_1}), \quad i = 2, \dots, d. \quad (14)$$

for some $\sigma^2 > 0$. The variable X_1 controls the variance of the other variables $X_{2:d}$. In particular, when X_1 takes large positive values, the variance of the remaining components becomes large and, conversely, for negative values, it becomes small, creating a *funnel-shaped* geometry in the joint distribution, see Figure 2, left panel. This structure makes the distribution challenging for sampling algorithms, in particular for popular gradient-based methods such as MALA and HMC, due to the light tails in the x_1 direction and irregular geometry.

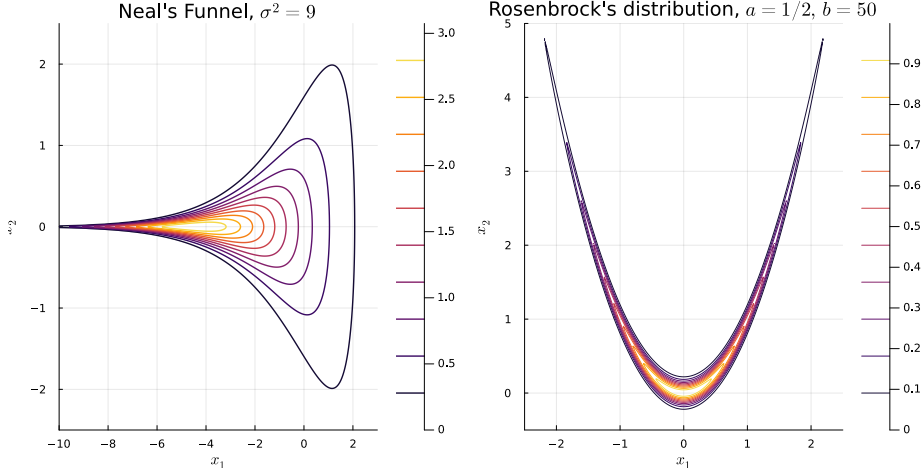


Fig. 2 Contour plots of a 2 dimensional Neal's Funnel target with $\sigma^2 = 9$ (left panel) and a 2 dimensional Rosenbrock's banana distribution with $a = 1/2, b = 50$ (right panel).

In all experiments, the step size h_i at iteration i is adaptively tuned as in [Andrieu and Thoms \(2008\)](#), that is, at iteration i , the step size is updated as

$$\log h_{i+1} = \log h_i + i^{-\beta}(\alpha_i - \alpha^*) \quad (15)$$

where α_i is the acceptance probability computed at iteration i , $\beta = 0.6$ is a learning parameter and $\alpha^* \in (0, 1)$ is the target probability which is set to be equal to the optimal acceptance rates derived in Section 4, Table 1.

The left panel of Figure 3 shows the histograms and Q-Q plots of the first component x_1 obtained with $N = 10^6$ samples of standard MALA and Auxiliary-variable MALA with Uniform and Exponential randomized step sizes targeting a $d = 10$ Neal's Funnel in (14) with $\sigma^2 = 9$. For all Markov chains we set the same starting value $X_0 \sim \mathcal{N}(0, I_{d \times d})$, a burn in equal to $N/10$ iterations and an initial step size equal to 1. Standard MALA fails to explore the neck of the funnel, i.e. the left tail of the first component, but the randomized versions appear to explore this region better.

The right panel of Figure 3 shows the estimation of $\mathbb{P}(X_1 < \xi_{0.05})$, where $\xi_{0.05}$ is the 5th percentile, as the number of iterations of the algorithm increases. The box-plots are obtained with 20 independent runs of the Markov chains targeting (14) with $\sigma^2 = 4$. Note that, for standard MALA, the upper and lower quantiles are equal to 0 in all experiments, meaning that the majority of the MCMC runs failed to reach values below $\xi_{0.05}$ on their first component.

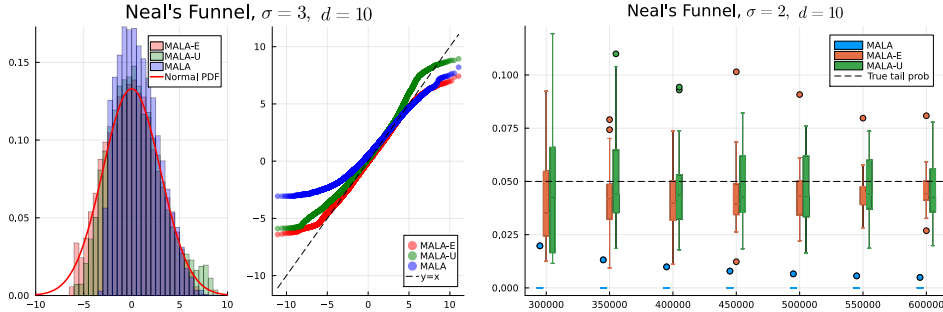


Fig. 3 Left panel: histograms and Q-Q plots of the first components x_1 for MALA (blue) and Auxiliary-variable MALA with Uniform (green) and Exponential (red) randomized step sizes. The red solid line shows the true marginal density of X_1 . Right panel: box plots for the estimation $\mathbb{P}(X_1 < \xi_{0.05})$ over 20 independent simulations of each algorithm, as the number of iterations (x -axis) increases.

5.3 The Rosenbrock distribution

The two-dimensional Rosenbrock distribution is defined as

$$X_1 \sim \mathcal{N}\left(0, \frac{1}{2a}\right), \quad X_2 | X_1 \sim \mathcal{N}\left(X_1^2, \frac{1}{2b}\right) \quad (16)$$

for parameters $a > 0$ and $b > 0$. The nonlinear dependence between X_1 and X_2 produces a curved, banana-shaped density, see Figure 2, right panel.

We perform similar experiments as in Section 5.2, where the step size h is adaptively tuned as in (15). Figure 4, left panel, shows the histograms and Q-Q plots of the first component obtained with $N = 2 \times 10^6$ samples of MALA and Auxiliary-variable MALA with Exponential and Uniform randomized step sizes targeting (16) with $a = 1/2$, $b = 50$. Initialization and burn in are set as in Section 5.2. The right-hand side shows the estimation of $\mathbb{P}(|X_1| > \xi_{0.95})$ for the same target, where $\xi_{0.95}$ is the 95th percentile, as the number of iterations increases. The box plots are again obtained with 20 independent runs of each algorithm.

The results suggest that the Auxiliary-variable MALA algorithms improve the exploration of the tails, although the differences in performance with respect to standard MALA are less dramatic compared with Section 5.2.

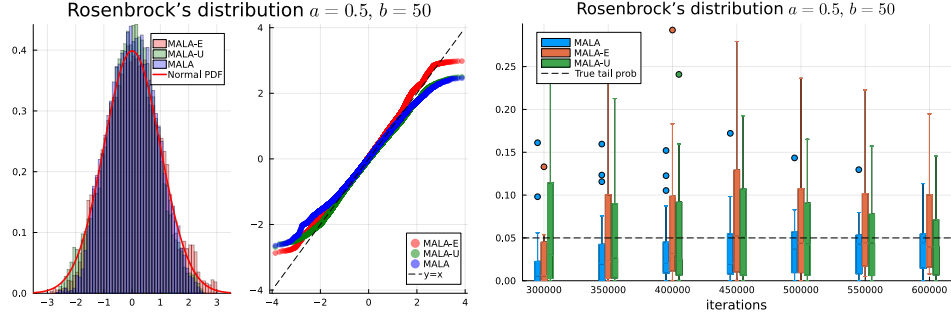


Fig. 4 Left panel: same as in Figure 3. Right panel: box plots for the estimation $\mathbb{P}(|X_1| > \xi_{0.95})$ over 20 independent simulations of each algorithm, as the number of iterations increases (x -axis).

5.4 Poisson regression model

For $i = 1, 2, \dots, n$, consider a regression model given by

$$Y_i \mid z_i \stackrel{\text{i.i.d.}}{\sim} \text{Poiss}(\exp(\langle z_i, x \rangle)), \quad (17)$$

with unknown parameter $x \in \mathbb{R}^d$ and sample size $n = 10d$. We set $d = 50$, $x \sim \mathcal{N}(0, I_{d \times d})$ and we simulate synthetic covariates $z_i \sim \mathcal{N}(0, I_{d \times d}/d)$ and Y_i from (17) for $i = 1, 2, \dots, n$. The posterior distribution π , given by the product of the likelihood and a standard Gaussian prior on x , is such that $\log \pi$ decays exponentially fast in the tails, creating a challenging target in particular at the tails of the distribution. Figure 5 shows the traces of MALA and our Auxiliary-variable algorithms, with adaptive step size as in (15). All algorithms were initialized in the tail of the distribution at $X_0 \sim \mathcal{N}(0, 10^2 \cdot I_{d \times d})$. The Auxiliary-variable algorithms appear to reach the bulk of the distribution faster than standard MALA.

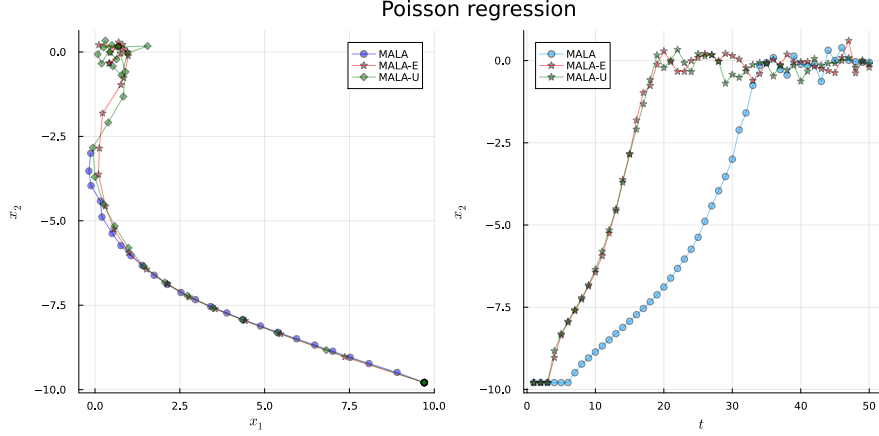


Fig. 5 Convergence of MALA (blue) and Auxiliary-variable MALA with Uniform (green) and Exponential (red) randomized step sizes initialized in the tails of the distribution. Left panel: trajectories of the first two coordinates. Right panel: traces of the first coordinate.

6 Discussion

We have shown how the randomization of a single one-dimensional parameter within a Metropolis–Hastings kernel can bring surprising benefits in terms of practical performance, and provided some novel theoretical results to explain this phenomenon. A natural extension is to consider the randomization of vector- or matrix-valued parameters. One obvious example is to randomize either a diagonal or dense preconditioning matrix. The recent work of [Hird and Livingstone \(2025\)](#) highlights scenarios in which spectral gaps and mixing times can be improved through the careful choice of a fixed matrix to precondition sampling algorithms, which is a popular element of the applied sampling toolkit, but little consideration has been given to the idea of randomizing this matrix at each iteration of the algorithm by sampling from some appropriate distribution. Indeed, in the case that this matrix is diagonal, the multi-dimensional Gaussian random walk Metropolis and Barker proposal algorithms can again be viewed as marginalized versions of simpler base kernels analogous to the one-dimensional scenario described in Section 2.3. Another natural question concerning kernels with a randomized step size such as \bar{P}_h and M_h is the optimal choice of μ , the randomizing distribution. Related questions concerning the optimal choice of proposal noise in the random walk Metropolis and Barker proposal have been considered previously in [Vogrinc et al. \(2023\)](#); [Neal and Roberts \(2011\)](#), but there are many ways in which such a question can be tackled and undoubtedly more to be learned. We leave a thorough exploration of these topics for future work.

We note in passing that a version of Hamiltonian Monte Carlo with a modified kinetic energy, as studied in [Livingstone et al. \(2019b\)](#); [Zhang et al. \(2016\)](#), combined with a randomized step size, produces a marginalized algorithm which is very close to the Barker proposal scheme of [Livingstone and Zanella \(2022\)](#) in one dimension. In the case that the kinetic energy is $|p|$, meaning the augmented momentum variable p follows a Laplace distribution, then a Hamiltonian proposal with a single leapfrog

step takes the form

$$x' = x + h \operatorname{sign} \left(p_0 + \frac{h}{2} (\log \pi)'(x) \right).$$

If h is then randomized using a half-Normal distribution, straightforward calculations show that the associated proposal density Q_h becomes

$$Q_h(x, y) = 2F_L \left((\log \pi)'(x) \frac{y - x}{h} \right) \mu \left(\frac{y - x}{h} \right),$$

where F_L denotes the cumulative distribution function (CDF) of the Laplace distribution. This represents a skew-symmetric distribution as described in [Azzalini \(2013\)](#), and differs from the Barker proposal only in the choice of CDF, which is instead taken from the logistic distribution in the Barker case, for reasons outlined in [Hird et al. \(2020\)](#); [Livingstone et al. \(2025\)](#). A version of this algorithm with multiple leapfrog steps would therefore be of interest, in combining the robustness of Barker and of the randomized kernels with the advantages of methods with auxiliary momentum like Hamiltonian Monte Carlo. Again we leave a detailed exploration for future work.

Acknowledgement

SG acknowledges support from the European Research Council (ERC), through the Starting grant ‘PrSc-HDBayLe’, project number 101076564. SL thanks Karan Garg for preliminary numerical work related to Section 5 during his MSc project at UCL.

References

Andrieu C, Livingstone S (2021) Peskun-Tierney ordering for Markovian Monte Carlo: beyond the reversible scenario. *Ann Statist* 49(4):1958–1981. <https://doi.org/10.1214/20-aos2008>, URL <https://doi.org/10.1214/20-aos2008>

Andrieu C, Thoms J (2008) A tutorial on adaptive mcmc. *Statistics and computing* 18:343–373

Andrieu C, Lee A, Vihola M (2018) Uniform ergodicity of the iterated conditional smc and geometric ergodicity of particle gibbs samplers. *Bernoulli* pp 842–872

Andrieu C, Lee A, Power S, et al (2022) Comparison of markov chains via weak poincaré inequalities with application to pseudo-marginal mcmc. *The Annals of Statistics* 50(6):3592–3618

Azzalini A (2013) The skew-normal and related families, vol 3. Cambridge University Press

Beskos A, Pillai N, Roberts G, et al (2013) Optimal tuning of the hybrid Monte Carlo algorithm. *Bernoulli* 19(5A):1501–1534. <https://doi.org/10.3150/12-BEJ414>, URL <https://doi.org/10.3150/12-BEJ414>

Durmus A, Moulines E, Saksman E (2020) Irreducibility and geometric ergodicity of Hamiltonian Monte Carlo. *Ann Statist* 48(6):3545–3564. <https://doi.org/10.1214/19-AOS1941>, URL <https://doi.org/10.1214/19-AOS1941>

Hastings WK (1970) Monte Carlo sampling methods using Markov chains and their applications. *Biometrika* 57(1):97–109. <https://doi.org/10.1093/biomet/57.1.97>, URL <https://doi.org/10.1093/biomet/57.1.97>

Hird M, Livingstone S (2025) Quantifying the effectiveness of linear preconditioning in markov chain monte carlo. *Journal of Machine Learning Research* 26(119):1–51

Hird M, Livingstone S, Zanella G (2020) A fresh take on ‘barker dynamics’ for mcmc. In: International Conference on Monte Carlo and Quasi-Monte Carlo Methods in Scientific Computing, Springer, pp 169–184

Iguchi Y, Livingstone S, Nüsken N, et al (2024) Skew-symmetric schemes for stochastic differential equations with non-lipschitz drift: an unadjusted barker algorithm. arXiv preprint arXiv:240514373

Jorgensen B (2012) Statistical properties of the generalized inverse Gaussian distribution, vol 9. Springer Science & Business Media

Livingstone S, Zanella G (2022) The barker proposal: Combining robustness and efficiency in gradient-based mcmc. *Journal of the Royal Statistical Society Series B: Statistical Methodology* 84(2):496–523

Livingstone S, Betancourt M, Byrne S, et al (2019a) On the geometric ergodicity of Hamiltonian Monte Carlo. *Bernoulli* 25(4A):3109–3138. <https://doi.org/10.3150/18-BEJ1083>, URL <https://doi.org/10.3150/18-BEJ1083>

Livingstone S, Faulkner MF, Roberts GO (2019b) Kinetic energy choice in Hamiltonian/hybrid Monte Carlo. *Biometrika* 106(2):303–319. <https://doi.org/10.1093/biomet/asz013>, URL <https://doi.org/10.1093/biomet/asz013>

Livingstone S, Vasdekis G, Zanella G (2025) Foundations of locally-balanced markov processes. arXiv preprint arXiv:250413322

Metropolis N, Rosenbluth AW, Rosenbluth MN, et al (1953) Equation of state calculations by fast computing machines. *The journal of chemical physics* 21(6):1087–1092

Mira A, Geyer CJ (1999) Ordering monte carlo markov chains. Tech. rep., University of Minnesota

Neal P, Roberts G (2011) Optimal scaling of random walk metropolis algorithms with non-gaussian proposals. *Methodology and Computing in Applied Probability* 13(3):583–601

Neal RM (2011) MCMC using Hamiltonian dynamics. In: Brooks S, Gelman A, Jones GL, et al (eds) *Handbook of Markov Chain Monte Carlo*. Chapman and Hall/CRC, chap 5, p 113–162

Pagani F, Wiegand M, Nadarajah S (2022) An n-dimensional rosenbrock distribution for markov chain monte carlo testing. *Scandinavian Journal of Statistics* 49(2):657–680

Peskun PH (1973) Optimum monte-carlo sampling using markov chains. *Biometrika* 60(3):607–612

Riou-Durand L, Vogrinc J (2022) Metropolis adjusted langevin trajectories: a robust alternative to hamiltonian monte carlo. arXiv preprint arXiv:220213230

Roberts GO, Rosenthal JS (1998) Optimal scaling of discrete approximations to Langevin diffusions. *J R Stat Soc Ser B Stat Methodol* 60(1):255–268. <https://doi.org/10.1111/1467-9868.00123>, URL <https://doi.org/10.1111/1467-9868.00123>

Roberts GO, Rosenthal JS (2001) Optimal scaling for various Metropolis-Hastings algorithms. *Statist Sci* 16(4):351–367. <https://doi.org/10.1214/ss/1015346320>, URL <https://doi.org/10.1214/ss/1015346320>

Roberts GO, Rosenthal JS (2004) General state space Markov chains and MCMC algorithms. *Probab Surv* 1:20–71. <https://doi.org/10.1214/154957804100000024>, URL <https://doi.org/10.1214/154957804100000024>

Roberts GO, Rosenthal JS (2016) Complexity bounds for markov chain monte carlo algorithms via diffusion limits. *Journal of Applied Probability* 53(2):410–420

Roberts GO, Tweedie RL (1996) Exponential convergence of Langevin distributions and their discrete approximations. *Bernoulli* 2(4):341–363. <https://doi.org/10.2307/3318418>, URL <https://doi.org/10.2307/3318418>

Roberts GO, Gelman A, Gilks WR (1997) Weak convergence and optimal scaling of random walk Metropolis algorithms. *Ann Appl Probab* 7(1):110–120. <https://doi.org/10.1214/aoap/1034625254>, URL <https://doi.org/10.1214/aoap/1034625254>

Rosenthal JS (2003) Asymptotic variance and convergence rates of nearly-periodic markov chain monte carlo algorithms. *Journal of the American Statistical Association* 98(461):169–177

Sherlock C, Roberts G (2009) Optimal scaling of the random walk metropolis on elliptically symmetric unimodal targets. *Bernoulli* pp 774–798

Storvik G (2011) On the flexibility of metropolis–hastings acceptance probabilities in auxiliary variable proposal generation. *Scandinavian Journal of Statistics* 38(2):342–358

Tierney L (1998) A note on metropolis-hastings kernels for general state spaces. *Annals of applied probability* pp 1–9

Titsias MK, Papaspiliopoulos O (2018) Auxiliary gradient-based sampling algorithms. *Journal of the Royal Statistical Society Series B: Statistical Methodology* 80(4):749–767

Vogrinc J, Livingstone S, Zanella G (2023) Optimal design of the barker proposal and other locally balanced metropolis–hastings algorithms. *Biometrika* 110(3):579–595

Yang J, Roberts GO, Rosenthal JS (2020) Optimal scaling of random-walk metropolis algorithms on general target distributions. *Stochastic Processes and their Applications* 130(10):6094–6132

Zhang Y, Chen C, Henao R, et al (2016) Laplacian hamiltonian monte carlo. In: *Joint European Conference on Machine Learning and Knowledge Discovery in Databases*, Springer, pp 98–114